

High-temperature relaxor ferroelectric behavior in Pr-doped SrTiO₃

Rajeev Ranjan,^{1,2} Rudi Hackl,³ Amreesh Chandra,⁴ Elmar Schmidbauer,⁵ Dmytro Trots,⁶ and Hans Boysen²

¹*School of Materials Science and Technology, Institute of Technology, Banaras Hindu University, Varanasi-221005, India*

²*Department für Geo-und Umweltwissenschaften, Sektion Kristallographie, Ludwig Maximilians Universität, Am Coulombwall 1, 85748 Garching, München, Germany*

³*Walther Meissner Institute, Bayerische Akademie der Wissenschaften, 85748 Garching, München, Germany*

⁴*Max Planck Institute for Polymer Research, Ackermannweg 10, 55128, Mainz, Germany*

⁵*Department of Earth and Environmental Sciences, Sektion Geophysik, Ludwig Maximilians Universität München, Theresienstr. 41, 80333 München, Germany*

⁶*Hasylab/DESY, Notkestr. 85, 22607 Hamburg, Germany*

(Received 20 July 2007; revised manuscript received 2 November 2007; published 20 December 2007)

Temperature-dependent Raman scattering, dielectric, and powder x-ray diffraction studies have been carried out on Pr-doped SrTiO₃ ceramic samples. Activation of TO₂ and TO₄ polar modes indicated increasing degree of polar distortion by Pr doping. Dielectric measurements revealed that the system exhibits dielectric relaxation peaks at ~500 K. The softening tendency of the polar TO₁ soft mode decreases with increasing Pr doping. X-ray diffraction results show no evidence of symmetry breaking across the dielectric peak temperatures. The system exhibits features of high-temperature relaxor ferroelectrics.

DOI: 10.1103/PhysRevB.76.224109

PACS number(s): 77.22.-d, 77.80.-e, 68.35.Rh, 63.20.-e

I. INTRODUCTION

SrTiO₃ (STO) has been a model system for understanding the mechanism of structural phase transitions in solids.¹ It is also a well known for its incipient ferroelectric and quantum paraelectric behavior at low temperatures.² The relative dielectric permittivity (ϵ_r') of bulk STO increases with decreasing temperature but saturates below 4 K presumably due to suppression of the ferroelectric state by zero-point quantum fluctuations of the lattice.² The ferroelectric state can, however, be stabilized by application of an external electric field,³ uniaxial stress,⁴ and also by chemical and isotopic substitutions.⁵⁻⁷ An unexpected onset of an intermediate antiferroelectric phase has also been reported for Ca substitution in STO.⁸⁻¹⁰ In most of the cases the ferroelectric ordering occurs well below room temperature. For example, the temperature corresponding to the dielectric permittivity anomalies (T_m) in Ca-substituted samples has been reported to be less than 35 K.⁵ In Bi-substituted STO, although dielectric relaxation peaks are reported at temperatures up to ~200 K, macroscopic polarization could survive only for temperatures less than 100 K.¹¹ High-temperature ferroelectric materials are of technological interest, and with increasing environmental concern, efforts are being made to search for more environmentally friendly lead-free ferroelectric materials. A possibility of stabilizing the ferroelectric phase at room temperature and above was theoretically predicted for biaxially strained STO¹² and was subsequently realized in a thin STO film grown on a DyScO₃ substrate.¹³ Durán *et al.*¹⁴ have recently reported the existence of a ferroelectric phase in Pr-doped SrTiO₃ ceramics even at room temperature. So far no detailed study in this regard has been reported. In order to have a better understanding of the development of the ferroelectric state in Pr-doped STO, we have carried out temperature-dependent Raman, dielectric, and x-ray diffraction measurements on this system. It is shown that the system exhibits dielectric relaxation around 500 K and the

ferroelectric state reported at room temperature therefore arises due to freezing of dynamic polar clusters around giant electric dipoles formed by Pr substitution.

II. EXPERIMENT

Ceramic specimens of Pr-doped SrTiO₃ were prepared as per the chemical formula Sr_{1-x}Pr_xTiO₃ with $x=0.025, 0.05,$ and 0.075 by the standard solid-state reaction method. Stoichiometric ratios of SrCO₃, TiO₂, and Pr₆O₁₁, each of purity greater than 99.9% (Alpha Aesar), were thoroughly mixed and calcined at 1100 °C for 3 h. The disk-shaped pellets were sintered at 1300 °C for 2 h. It may, however, be mentioned that Pr can exist in 3+ and 4+ valence states,¹⁴ and since the sizes of Pr³⁺ (1.126 Å) and Pr⁴⁺ (0.96 Å) lie between that of Sr²⁺ (1.44 Å) and Ti⁴⁺ (0.61 Å),¹⁵ a possibility of some fraction of the substituted Pr ions occupying the Ti site is also quite likely. In this paper, we have, however, not concerned ourselves with the problem of site occupancy of the substituted Pr ions in STO. Raman spectra were recorded on polished pellets in backscattering geometry. The samples were mounted on a heating stage with the temperature controllable in the range 300–800 K. The power of the Kr⁺ laser operated at 531 nm was set at 2 mW. The spectra were recorded with a Horiba Jobin Yvon T64000 triple spectrometer equipped with a liquid-N₂-cooled back-thinned charge-coupled-device (CCD) detector. High-resolution powder x-ray diffraction data were collected at HASYLAB (B2 beamline) at the synchrotron source (DESY) in Germany, using a wavelength of 0.798 09 Å (calibrated with a LaB₆ pattern). For dielectric measurements platinum electrodes were applied on cleaned surfaces of the disk-shaped sintered pellets. Capacitance and loss tangent were measured using a HP 4192 impedance analyzer.

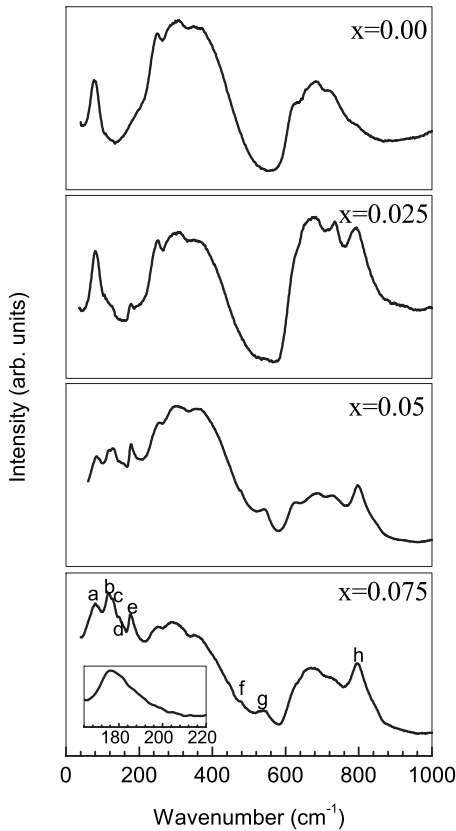


FIG. 1. Raman spectra of $\text{Sr}_{1-x}\text{Pr}_x\text{TiO}_3$ for $x=0.00, 0.025, 0.05,$ and 0.075 at 300 K. The inset in the lowest panel shows magnified plot in a limited frequency range. For convenience, the various modes are labeled in alphabetical order in the lowest panel (see text).

III. RESULTS AND DISCUSSION

A. Raman scattering at 300 K: Composition dependence

Figure 1 shows the Raman spectra of $\text{Sr}_{1-x}\text{Pr}_x\text{TiO}_3$ (SPT) for $x=0.00, 0.025, 0.05,$ and 0.075 . Apart from the two second-order broadbands centered around 300 and 700 cm^{-1} , distinct first-order modes are seen for all the compositions. These modes are labeled in alphabetical order *a–h* for $x=0.075$ in Fig. 1 and appear at 80 (*a*), 117 (*b*), 127 (*c*), 145 (*d*), 175 (*e*), 475 (*f*), 540 (*g*), and 795 (*h*) cm^{-1} . All these Raman modes are, in principle, forbidden by selection rules in the cubic phase of STO. Their occurrence is made possible by relaxation of these rules by unintentional and intentional structural defects. By comparison with previously published Raman and infrared scattering results on bulk STO^{16–21} and on thin STO films²² we identified the four Raman modes near 175, 475, 540, and 795 cm^{-1} as TO_2 , LO_3 , TO_4 , and LO_4 modes, respectively. The appearance of TO_2 and TO_4 modes, has been considered as evidence of polar nanoregions (PNRs) which characterize a relaxor ferroelectric system.^{16,23,24} The intensities of the TO_2 and TO_4 modes are more pronounced for the compositions $x=0.05$ and 0.075 than for $x=0.025$, suggesting increasing degree of polar distortion for the two higher compositions. The line shape of the TO_2 mode is strongly asymmetric and tails off on the high-

frequency side (see inset in the lowest panel of Fig. 1). This effect, known as the Fano effect, has also been reported in Ca-doped STO,¹⁶ thin STO film,²² and in doped KTaO_3 crystals.^{23,24}

A weak Raman mode at $\sim 145 \text{ cm}^{-1}$, visible in the spectra of the $x=0.05$ and 0.075 samples, corresponds to the hard structural E_g mode. This mode becomes visible in doped and undoped STO below the cubic-tetragonal antiferrodistortive (AFD) structural phase transition temperature.¹⁶ The AFD transition in STO is driven by softening and freezing of a triply degenerate R_{25} phonon at the R point of the cubic Brillouin zone.²⁵ The presence of this weak mode indicates local/global AFD distortion at room temperature. Local AFD distortions have also been reported at room temperature in the (globally) cubic phase of $\text{Sr}_{0.94}\text{Ca}_{0.06}\text{TiO}_3$,²⁶ as well as in Bi-doped STO.²⁷

A mode near 80 cm^{-1} is most pronounced for the compositions $x=0.00$ and 0.025 . This mode corresponds to an IR-active soft TO_1 mode^{3,17,19} which is known to exhibit a softening tendency.^{3,16} Porokhonsky *et al.*²⁷ have shown that doping of impurity ions considerably influences the frequency of this mode. Bi doping increases the mode frequency (at 300 K) to 103 cm^{-1} for 0.67 mol % Bi and to 126 cm^{-1} for 13.3 mol % of Bi. This hardening has been attributed to frequency shift of anharmonic oscillator biased by random electric fields of the dipole impurities. In contrast to Bi-doped STO, the frequency of this mode at 300 K is nearly composition independent in Pr-doped STO. Further, two new modes near 117 and 127 cm^{-1} are observed. Unlike the other modes mentioned above, these new modes are not likely to originate from disorder-induced activation of the modes of cubic STO. Their presence is suggestive of activation of local modes by Pr doping. Similar modes at ~ 261 and 520 cm^{-1} in Bi-doped STO have been attributed to originate from coupling of the dynamics off-centered Bi ions with the soft TO mode.²⁷

B. Raman scattering: Temperature dependence

Raman spectra as a function of temperature for all the three compositions were measured to understand the role of lattice dynamics in bringing about the ferroelectric state in Pr-doped STO. Figures 2 and 3 show Raman spectra of the samples with $x=0.025$ and 0.075 at selected temperatures. Of the various phonon modes mentioned above, only the lowest-energy phonon (TO_1) was found to be sensitive to changes in temperature. The hard polar modes TO_2 and TO_4 in doped incipient ferroelectrics such as STO and KTaO_3 have been used to characterize the PNRs.^{23,24,28} The intensity of the TO_2 mode in $\text{Sr}_{0.993}\text{Ca}_{0.007}\text{TiO}_3$ ($T_m \sim 18 \text{ K}$) has been related to the space and time autocorrelation $\langle P^2 \rangle$ of the fluctuating impurity-induced polarization $P(r, t)$.²⁸ The intensity of the TO_2 mode in Pr-doped STO persisted on heating up to 773 K, which is $\sim 280 \text{ K}$ above the temperature of the dielectric anomaly ($T_m \sim 500 \text{ K}$), without any appreciable change. This suggests that the polar regions in Pr-doped STO persist up to 773 K and presumably even higher.

Figures 4(a) and 4(b) show magnified plots of the TO_1 mode of $\text{Sr}_{0.95}\text{Pr}_{0.05}\text{TiO}_3$ and $\text{Sr}_{0.925}\text{Ca}_{0.075}\text{TiO}_3$, respectively,

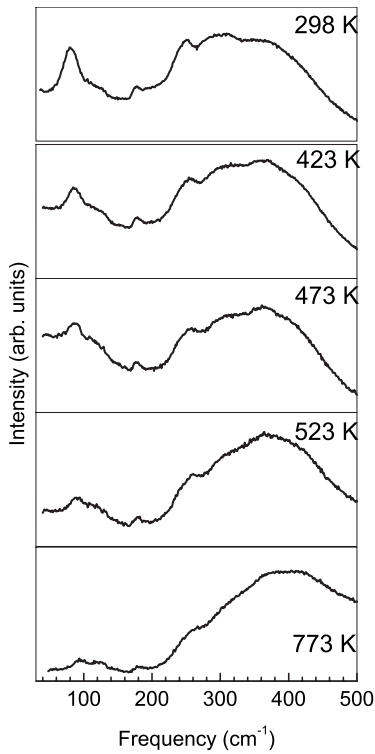


FIG. 2. Raman spectra of $\text{Sr}_{0.975}\text{Pr}_{0.025}\text{TiO}_3$ at various temperatures

at three representative temperatures. The change in frequency of this mode with temperature is evident for $x=0.05$. For $x=0.075$, the frequency of this mode is independent of temperature [Fig. 4(b)]. Figure 5 shows a typical variation of the frequency of the TO_1 mode of $x=0.025$ with temperature. The frequency of this mode changes by 15 cm^{-1}

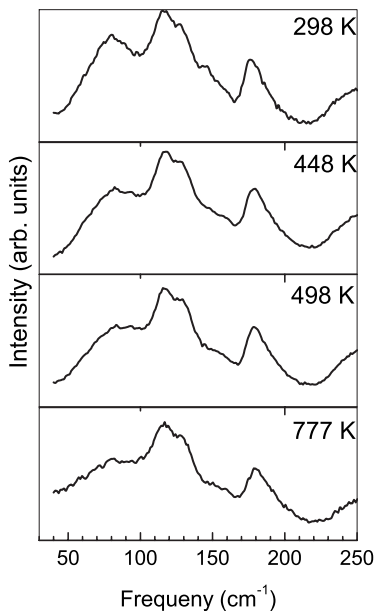


FIG. 3. Raman spectra of $\text{Sr}_{0.925}\text{Pr}_{0.075}\text{TiO}_3$ at various temperatures

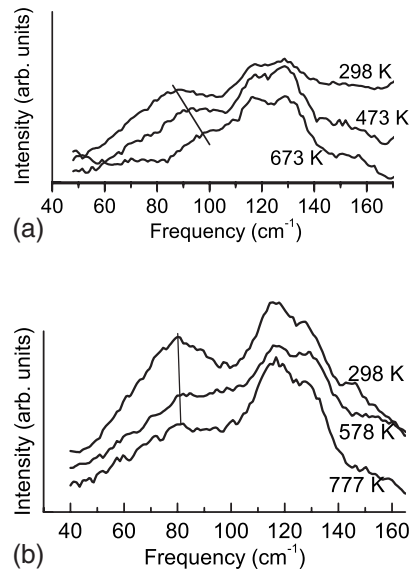


FIG. 4. Magnified plot of TO_1 mode of (a) $\text{Sr}_{0.95}\text{Pr}_{0.05}\text{TiO}_3$ and (b) $\text{Sr}_{0.925}\text{Pr}_{0.075}\text{TiO}_3$ at three representative temperatures. The TO_1 mode retains its softening tendency in (a) while it is almost temperature independent in (b).

on varying the temperature from 298 K to 773 K. The softening ability of the TO_1 mode gradually decreases with increasing the Pr content as is evident from Fig. 6 which depicts the total change in frequency on heating from 300 K to 773 K for the three compositions. For $x=0.075$, the TO_1 mode behaves like a hard mode. Similar behavior was reported in Ref. 27 for Bi-doped STO. A comparison of results with Bi-doped STO suggests that the stiffening tendency of the soft TO_1 mode is more enhanced in Pr-doped STO specimens. For example, for 0.67 mol % Bi-doped STO, the mode frequency has been reported to change from 103 cm^{-1} at 300 K to 86 cm^{-1} at 260 K—i.e., a shift of 17 cm^{-1} on changing the temperature by merely 40 K.²⁷ The softening behavior of the TO_1 mode in Bi-doped STO, though reduced on increasing the Bi concentration, survives even for 13.3 mol % of Bi doping and continues well below T_m .²⁷ Thus, unlike for the lightly Ca-doped STO ($\text{Sr}_{0.993}\text{Ca}_{0.007}\text{TiO}_3$, $T_m \sim 18 \text{ K}$),²⁸ where it has been shown that the TO_1 mode hardens below T_m and splits into three components, thereby lowering the symmetry of the system from tetragonal to orthorhombic,¹⁶ the soft mode is not hard-

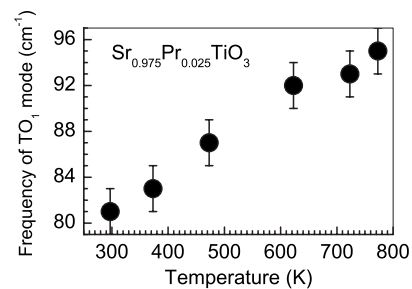


FIG. 5. Temperature variation of frequency of the TO_1 mode of $\text{Sr}_{0.975}\text{Pr}_{0.025}\text{TiO}_3$.

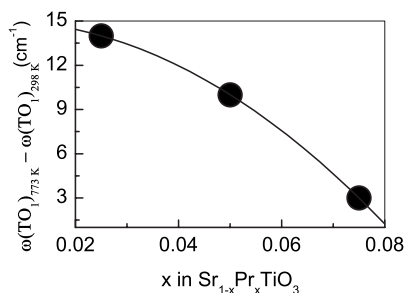


FIG. 6. Variation of the difference of the frequency of the TO_1 mode at 298 K and 773 K with composition. The graph shows that Pr doping gradually decrease the softening ability of the TO_1 mode.

ened below their respective T_m 's of Pr- and Bi-doped STO ($x=0.025, 0.05$). As a result, a symmetry change across T_m is less likely in the latter systems. All this evidence suggests that the dielectric anomalies reported in the Pr-doped STO samples¹⁴ cannot be due to a displacive ferroelectric phase transition.

C. Dielectric response

Having shown in the previous section that the reported dielectric anomalies in Pr-doped STO are not related to displacive ferroelectric transition, we investigated the dielectric behavior of the Pr-doped STO ceramic pellets as a function of temperature at various frequencies of the measuring ac signal. Figure 7 shows the real (ϵ_r') and imaginary (ϵ_r'') parts of the relative dielectric permittivity as a function of temperature at different frequencies. Two features worth noting are that (i) for a given frequency, the imaginary part peaks at

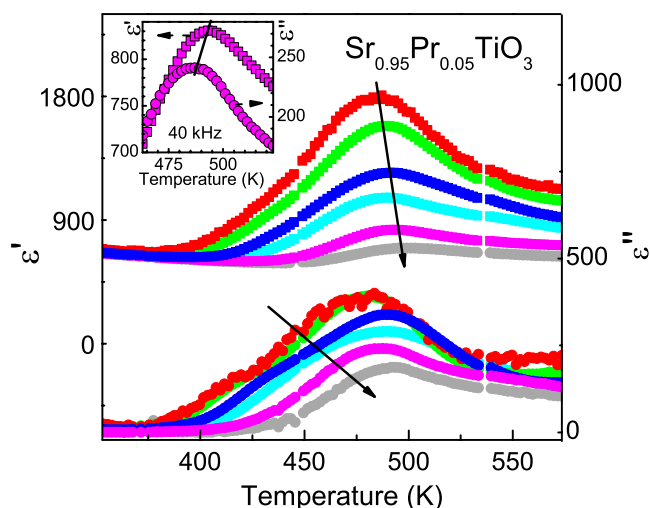


FIG. 7. (Color online) Temperature variation of real (upper plots) and imaginary parts (lower plots) of the relative dielectric permittivity at various frequencies: (a) 0.4 kHz, (b) 1 kHz, (c) 4 kHz (d) 10 kHz, (e) 40 kHz, and (f) 100 kHz. The arrows indicate the direction of increasing frequency. The inset shows magnified plot of the real and imaginary parts of relative permittivity at 40 kHz.

lower temperature than the real part (see inset of Fig. 7) and (ii) the peak temperature of both ϵ_r' and ϵ_r'' shifts to higher temperature with increasing frequency of the measuring signal. The permittivity peaks therefore correspond to dielectric relaxation and not a phase transition. This is consistent with the Raman results reported in the previous section. Further, the fact that this composition exhibits polarization–electric-field (P - E) hysteresis loop characteristic of a ferroelectric state, at room temperature,¹⁴ suggests that the observed dielectric relaxation is a manifestation of relaxor ferroelectric behavior.^{29,30} Relaxor ferroelectric behavior below room temperature has also been reported in Bi-doped STO.¹¹ An attempt to fit Vogel-Fulcher relationship to the peak temperatures (obtained by visual inspection) at different frequencies was however unsuccessful. A close inspection of the shape of the peaks revealed that more than one relaxation processes is at play. In this context it is interesting to note that the dielectric relaxation above room temperature in the imaginary part of permittivity, attributed to Maxwell-Wagner relaxation, has been reported even in pure STO ceramics.³¹ The asymmetric relaxation peaks in the imaginary part of the permittivity observed in Pr-doped STO can therefore have contributions from the Maxwell-Wagner process as well. Further, in the present case, since divalent Sr^{2+} is replaced by Pr which can exist in 3+ as well as 4+ states, strontium and oxygen vacancies will be created to satisfy charge neutrality. The existence of Pr^{3+} and Pr^{4+} valence states at the Sr sites and formation of $Pr^{3+}/Pr^{4+}-V_{Sr}$ centers responsible for setting up random (local) electric field and/or strain fields has been proposed in Ref. 14. Such a random field can induce a ferroelectric domain state and give rise to a relaxor ferroelectric behavior.³²

As far as our present understanding is concerned, the development of a ferroelectric state in doped incipient ferroelectric systems is intimately related to the formation of PNRs around the defect sites, the size of which grow on approaching T_m from the high-temperature side due to coupling with the soft ferroelectric mode. In this scenario, the size of a PNR should be determined by the magnitude of the dipole moment of the dipolar species in the host matrix. At any given temperature, a dipole with larger moment will polarize the surrounding host matrix more than a dipole with smaller moment. Since the dielectric permittivity of STO is considerably lower above room temperature as compared to its value at low temperatures,² freezing of polar clusters above room temperature and consequent development of a ferroelectric state suggests the presence of dipolar species with giant dipole moments at the defect sites. These giant dipoles are able to create polar clusters (PNRs) of sufficiently large size even at high temperatures such that they can overlap and eventually lead to the development of a ferroelectric state. In analogy with the previous studies on Ca-doped STO,³² the smaller size of Pr^{3+} (1.126 Å) and Pr^{4+} (0.96 Å) than that of Sr^{2+} (1.44 Å) can cause Pr^{3+}/Pr^{4+} to take up off-centered positions and create electric dipoles around which PNRs can develop. Alternatively, it is also possible for Ti^{4+} near a Pr site to take up an off-centered position, resulting in local ferroelectric distortions, due to favorable hybridization between Ti d orbitals and O $2p$ orbitals³³ assisted by local strain induced by size mismatch between the host and guest ions. Skanavi *et al.* have considered hop-

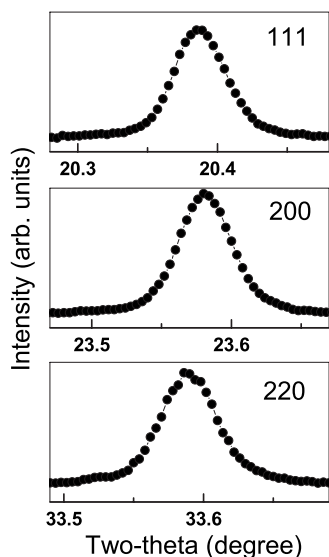


FIG. 8. Powder x-ray diffraction profiles of (a) {111}, (b) {200}, and (c) {220} cubic Bragg reflections of $\text{Sr}_{0.95}\text{Pr}_{0.05}\text{TiO}_3$.

ping of off-centered Ti^{4+} to explain the dielectric relaxation in Bi-doped STO.³⁴ Local structure study can reveal the correct picture among these plausible models.

D. X-ray powder diffraction

In order to investigate whether or not the development of the ferroelectric state is accompanied by breaking of the global symmetry we carried out high resolution powder x-ray diffraction at room temperature for all the compositions mentioned above. Since STO is cubic ($Pm\bar{3}m$) at 300 K, all the Bragg peaks must be singlet. Any distortion of the cubic lattice would result in the development of an asymmetry or splitting of the some of the Bragg reflections. Figure 8 shows selected profiles corresponding to the Bragg reflections {111}, {200}, and {220} of $\text{Sr}_{0.95}\text{Pr}_{0.05}\text{TiO}_3$ at room temperature. It is evident from this figure that all the profiles are singlets, thereby suggesting that there is no noticeable distortion of the cubic lattice in the ferroelectric state. The present

case is more akin to the well-known high-temperature relaxor $\text{PbMg}_{1/3}\text{Nb}_{2/3}\text{O}_3$ (PMN), and Li-doped KTaO_3 (for Li concentration less than 5 mol %) systems. Both systems do not exhibit features of global symmetry breaking below their respective T_m 's.^{35–37}

IV. CONCLUSIONS

To summarize, we have shown that Pr doping in SrTiO_3 ($\text{Sr}_{1-x}\text{Pr}_x\text{TiO}_3$) exhibits dielectric anomalies around 500 K, a temperature which is considerably large than those reported for other impurity systems in STO. The polar TO_1 mode behaves differently for different compositions. For $x=0.025$ and 0.05 it behaves like a soft mode while it is almost temperature independent for $x=0.075$. The softening behavior in the first two compositions continues well below T_m , suggesting that the dielectric anomalies in this system and the related development of ferroelectric state below T_m are not due to a displacive ferroelectric phase transition proposed earlier. The global structure of the system well below the permittivity anomaly temperature (T_m) remains cubic, suggesting that the global lattice distortion in the ferroelectric state is insignificant. Detailed dielectric measurements have revealed that the dielectric anomalies are related to relaxational freezing of PNRs similar to other relaxor ferroelectric systems. It is proposed that Pr doping induces “giant electric dipoles” which are able to polarize the SrTiO_3 matrix around them and lead to their cooperative freezing without the need to lower the temperature of the system well below 300 K. The results are expected to stimulate further research in this direction and may lead to the discovery of other systems based on doped STO which exhibit ferroelectric behavior at high temperatures that may have important technological implications.

ACKNOWLEDGMENTS

This work was supported by the Department of Science and Technology, Government of India. R.R. is grateful to the Alexander von Humboldt foundation for support during a stay in Germany during which part of this work was carried out.

¹A. D. Bruce and R. A. Cowley, *Adv. Phys.* **29**, 219 (1980).

²K. A. Müller and H. Burkard, *Phys. Rev. B* **19**, 3593 (1979).

³P. A. Fleury and J. M. Worlock, *Phys. Rev.* **174**, 613 (1968).

⁴H. Uwe and T. Sakudo, *Phys. Rev. B* **13**, 271 (1976).

⁵J. G. Bednorz and K. A. Müller, *Phys. Rev. Lett.* **52**, 2289 (1984).

⁶V. V. Lemanov, E. P. Smirnova, P. P. Syrnikov, and E. A. Taranov, *Phys. Rev. B* **54**, 3151 (1996).

⁷M. Itoh, R. Wang, Y. Inaguma, T. Yamaguchi, Y.-J. Shan, and T. Nakamura, *Phys. Rev. Lett.* **82**, 3540 (1999).

⁸R. Ranjan, D. Pandey, and N. P. Lalla, *Phys. Rev. Lett.* **84**, 3726 (2000).

⁹R. Ranjan and D. Pandey, *J. Phys.: Condens. Matter* **13**, 4239 (2001).

¹⁰R. Ranjan and D. Pandey, *J. Phys.: Condens. Matter* **13**, 4251 (2001).

¹¹Chen Ang, Zhi Yu, P. Lunkenheimer, J. Hemberger, and A. Loidl, *Phys. Rev. B* **59**, 6670 (1999).

¹²N. A. Pertsev, A. K. Tagantsev, and N. Setter, *Phys. Rev. B* **61**, R825 (2000).

¹³J. H. Haeni, P. Irvin, W. Chang, R. Uecker, P. Reiche, Y. L. Li, S. Choudhury, W. Tian, M. E. Hawley, B. Craigo, A. K. Tagantsev, X. Q. Pan, S. K. Streiffer, L. Q. Chen, S. W. Kirchoefer, J. Levy, and D. G. Schlom, *Nature (London)* **430**, 758 (2004).

¹⁴A. Durán, E. Martínez, J. A. Díaz, and J. M. Siqueiros, *J. Appl. Phys.* **97**, 104109 (2005).

¹⁵R. D. Shannon, *Acta Crystallogr., Sect. A: Cryst. Phys., Diffr.*

- Theor. Gen. Crystallogr. **32**, 751 (1976).
- ¹⁶U. Bianchi, W. Kleemann, and J. G. Bednorz, *J. Phys.: Condens. Matter* **6**, 1229 (1994).
- ¹⁷J. Petzelt, T. Ostapchuk, I. Gregora, I. Rychetský, S. Hoffmann-Eifert, A. V. Pronin, Y. Yuzyuk, B. P. Gorshunov, S. Kamba, V. Bovtun, J. Pokorný, M. Savinov, V. Porokhonskyy, D. Rafaja, P. Vaněk, A. Almeida, M. R. Chaves, A. A. Volkov, M. Dressel, and R. Waser, *Phys. Rev. B* **64**, 184111 (2001).
- ¹⁸V. N. Denisov, B. N. Mavrin, and V. B. Podobedov, *Phys. Rep.* **151**, 1 (1987).
- ¹⁹H. Vogt and G. Rossbroich, *Phys. Rev. B* **24**, 3086 (1981).
- ²⁰W. G. Nielsen and J. G. Skinner, *J. Chem. Phys.* **48**, 2240 (1968).
- ²¹A. S. Barker, Jr., *Phys. Rev.* **145**, 391 (1966).
- ²²A. A. Sirenko, I. A. Akimov, J. R. Fox, A. M. Clark, H. C. Li, W. Si, and X. X. Xi, *Phys. Rev. Lett.* **82**, 4500 (1999).
- ²³J. Toulouse, P. DiAntonio, B. E. Vugmeister, X. M. Wang, and L. A. Knauss, *Phys. Rev. Lett.* **68**, 232 (1992).
- ²⁴P. DiAntonio, B. E. Vugmeister, J. Toulouse, and L. A. Boatner, *Phys. Rev. B* **47**, 5629 (1993).
- ²⁵P. A. Fleury, J. F. Scott, and J. M. Worlock, *Phys. Rev. Lett.* **21**, 16 (1968).
- ²⁶S. K. Mishra, R. Ranjan, D. Pandey, P. Ranson, R. Ouillon, J. P. Lucarre, and P. Pruzan, *J. Solid State Chem.* **178**, 2846 (2005).
- ²⁷V. Porokhonskyy, A. Pashkin, V. Bovtun, J. Petzelt, M. Savinov, P. Samoukhina, T. Ostapchuk, J. Pokorny, M. Avdeev, A. Kholkin, and P. Vilarinho, *Phys. Rev. B* **69**, 144104 (2004).
- ²⁸U. Bianchi, J. Dec, W. Kleemann, and J. G. Bednorz, *Phys. Rev. B* **51**, 8737 (1995).
- ²⁹L. E. Cross, *Ferroelectrics* **76**, 241 (1987).
- ³⁰G. A. Samara, *J. Phys.: Condens. Matter* **15**, R367 (2003).
- ³¹H. Neumann and G. Arlt, *Ferroelectrics* **69**, 179 (1986).
- ³²W. Kleemann, *Int. J. Mod. Phys. B* **7**, 2469 (1993).
- ³³R. E. Cohen, *Nature (London)* **358**, 136 (1992).
- ³⁴G. I. Scanavi, I. J. Ksendzov, V. A. Trigubenko, and V. G. Prokhatilov, *Zh. Eksp. Teor. Fiz.* **33**, 320 (1957) [*Sov. Phys. JETP* **6**, 250 (1958)].
- ³⁵N. de Mathan, E. Husson, G. Calvarin, J. R. Gavarri, A. W. Hewat, and A. Morell, *J. Phys.: Condens. Matter* **3**, 8158 (1991).
- ³⁶S. R. Andrews, *J. Phys. C* **18**, 1357 (1985).
- ³⁷U. T. Hochli, K. Knorr, and A. Loidl, *Adv. Phys.* **39**, 405 (1990).